



Location:

Saltsburg, PA

©Michael Krzanowsky,

212 Lexington Ave.,

Johnstown, PA

USA

15902

ph: 1-814-539-5705

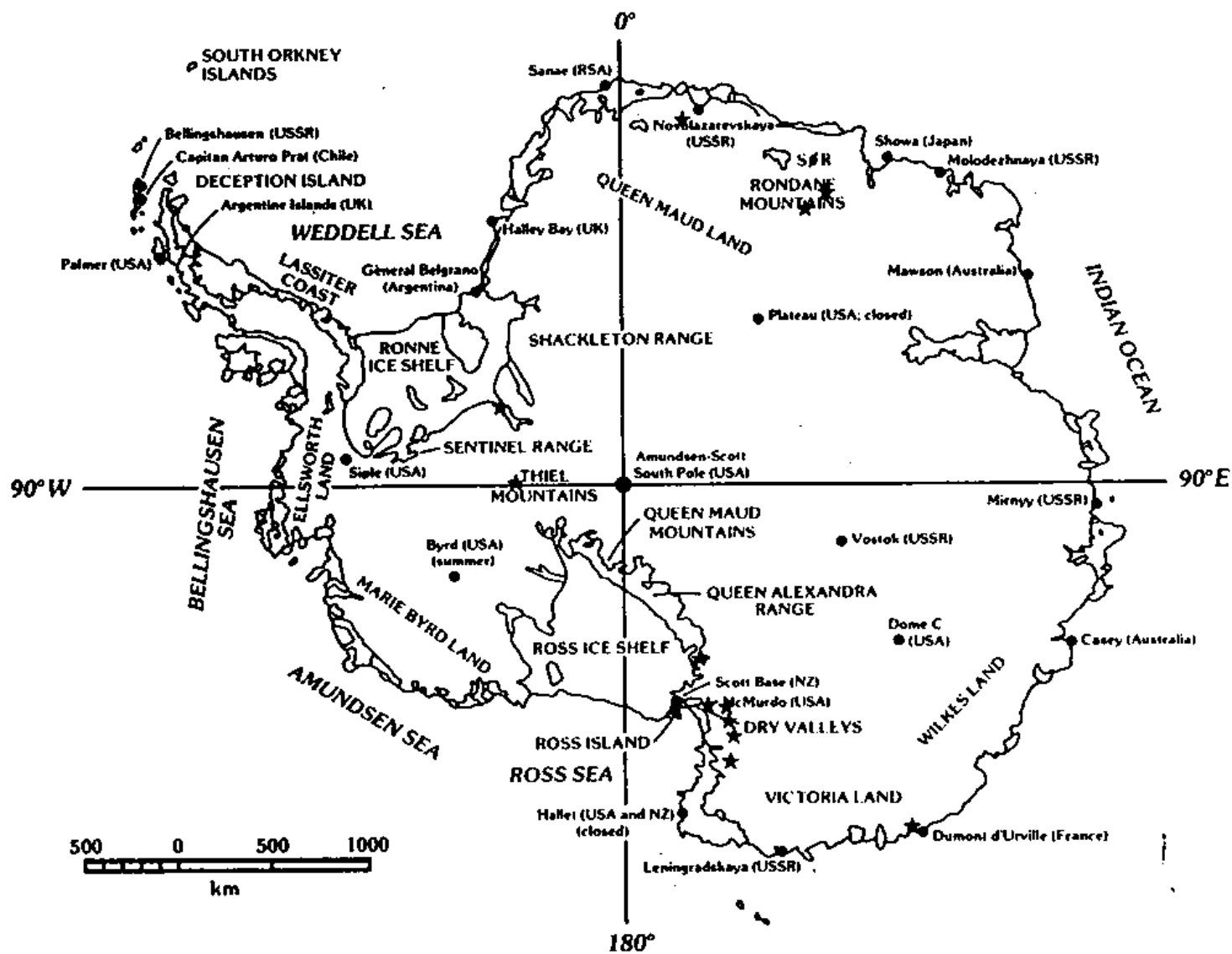


Fig. 1.11. Meteorite concentrations have been found in Antarctica in the Transantarctic Mountains near the Allan Hills (stars in Victoria Land) by USA scientific teams and in the Rondane Mountains near the Yamato Mountains (stars in Queen Maud Land) by Japanese expeditions. The individual meteorites recovered from these two areas in the last few years number in the thousands. Other areas such as the Thiel Mountains are expected to yield similar

Ice Movement and Meteorite Concentration

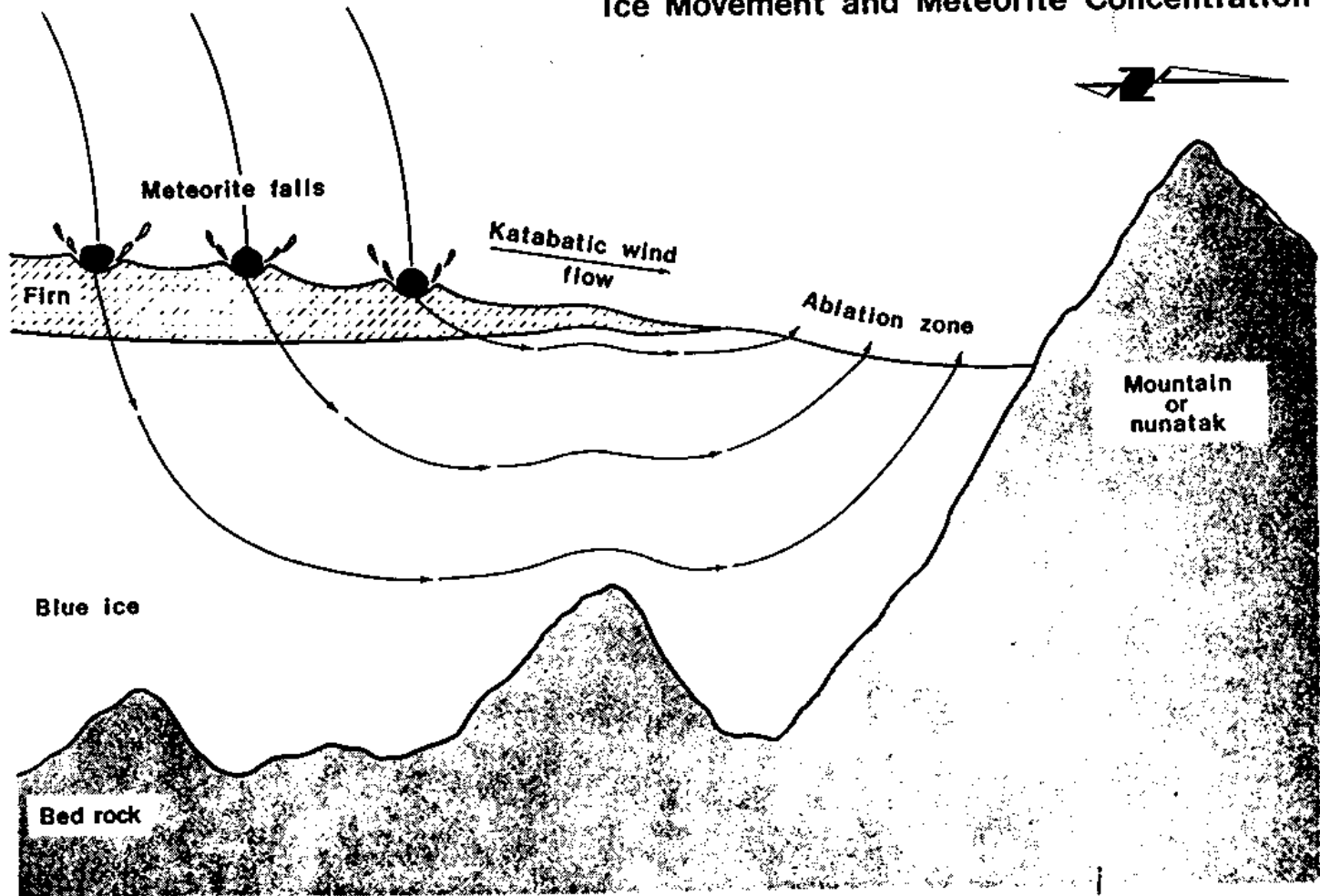
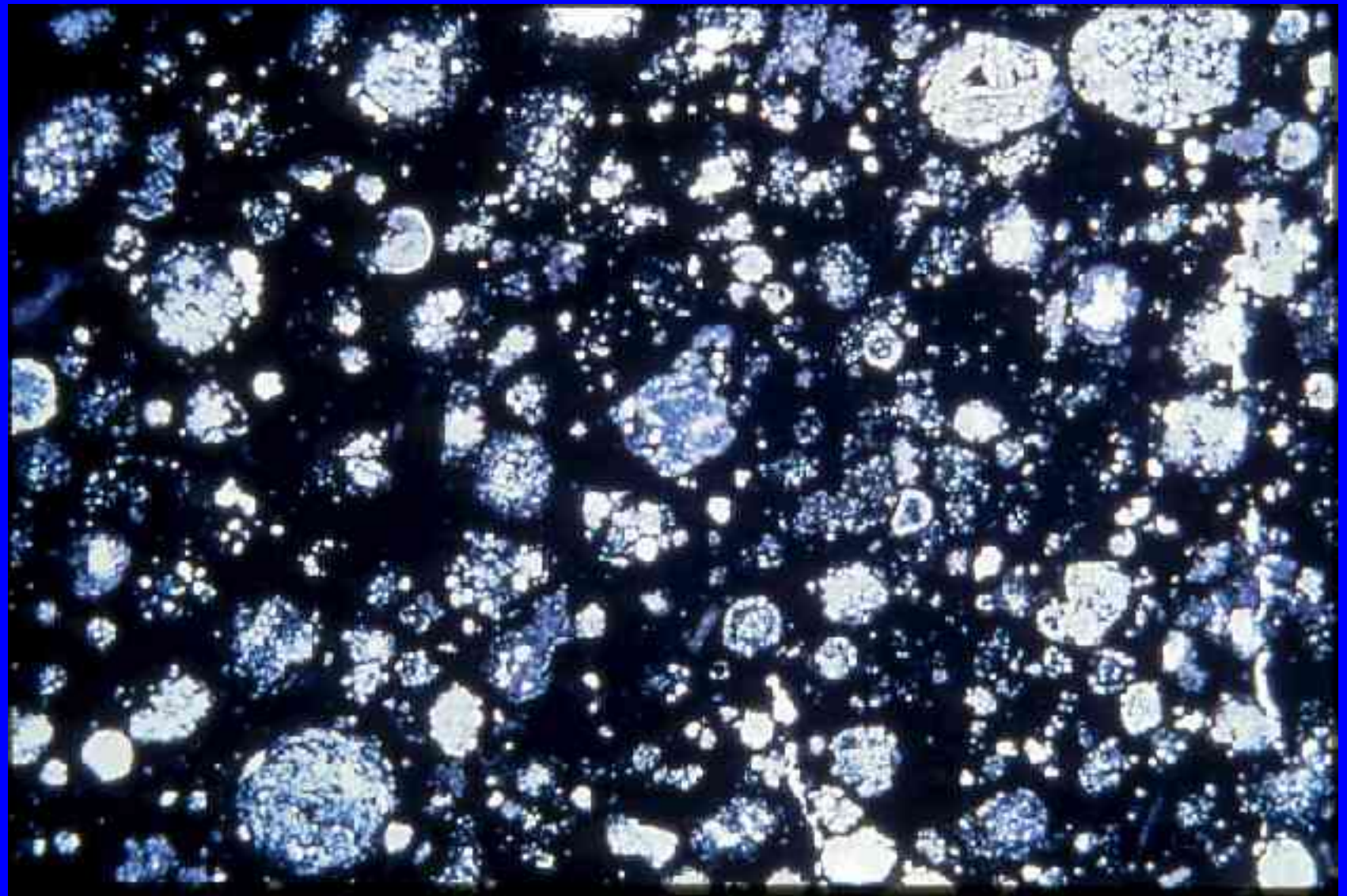


Fig. 1.13. This diagram schematically illustrates the meteorite concentration mechanism in the Allan Hills and possibly other locations in Antarctica. All over the continent, meteorites fall into firn and are ultimately frozen into the accumulating blue ice. The ice sheet flows outward toward the edges of the continent unless it meets an obstruction such as a nunatak. Stagnant ice behind such a barrier will undergo ablation by katabatic winds, and meteorites will accumulate as successive layers of ice are exposed and removed in this way. Courtesy of NASA.

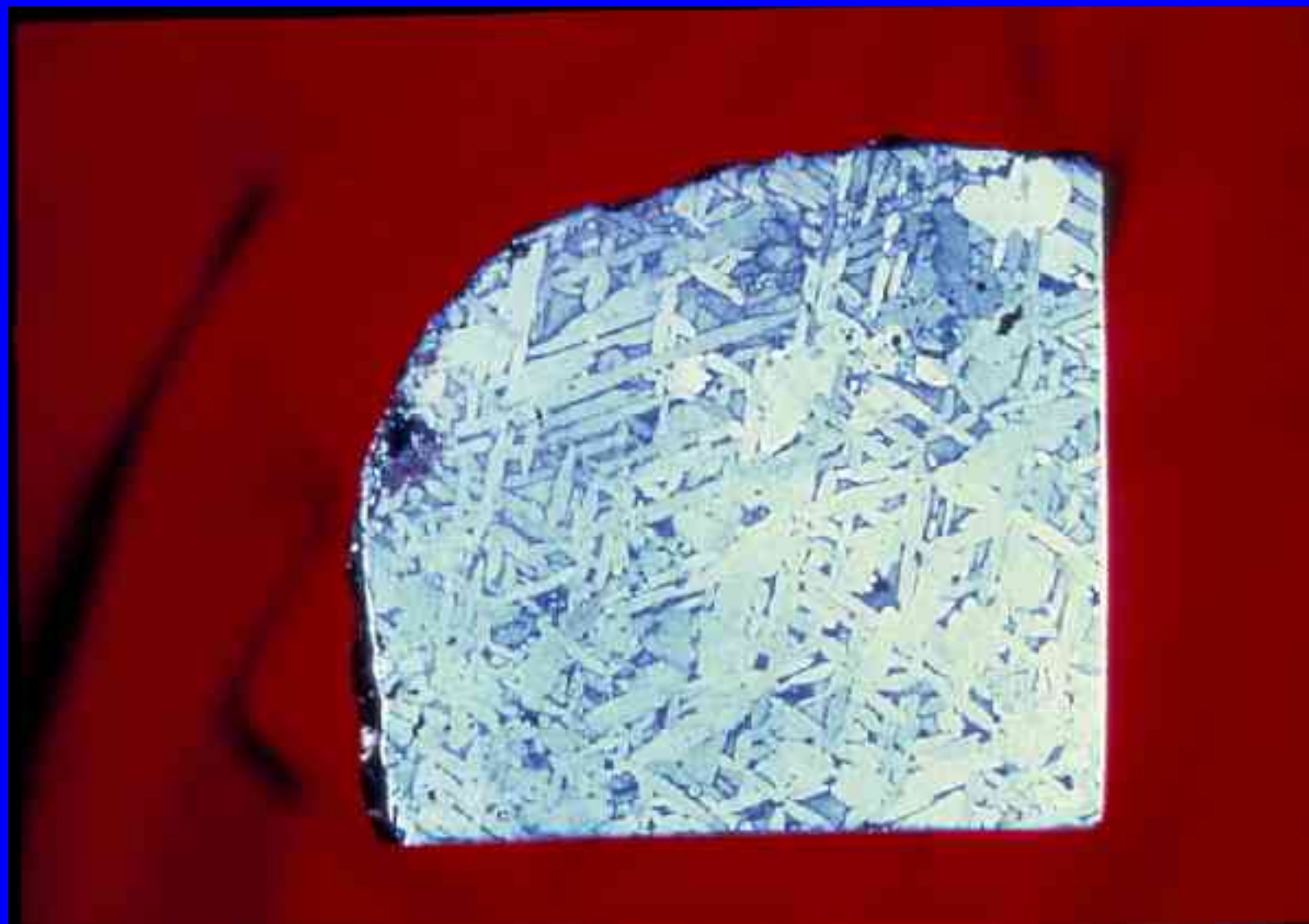


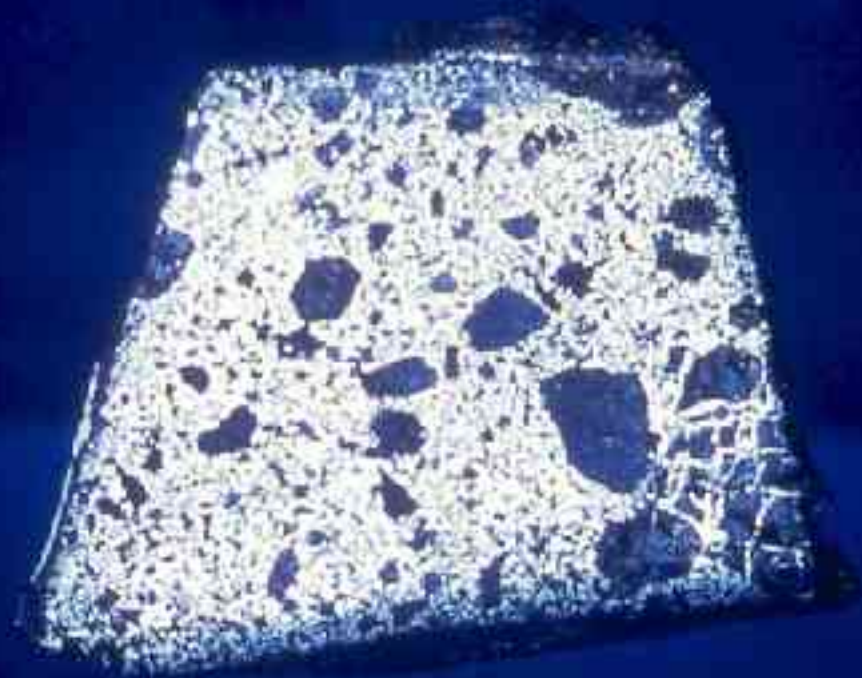












ALH84001,0

1cm
E



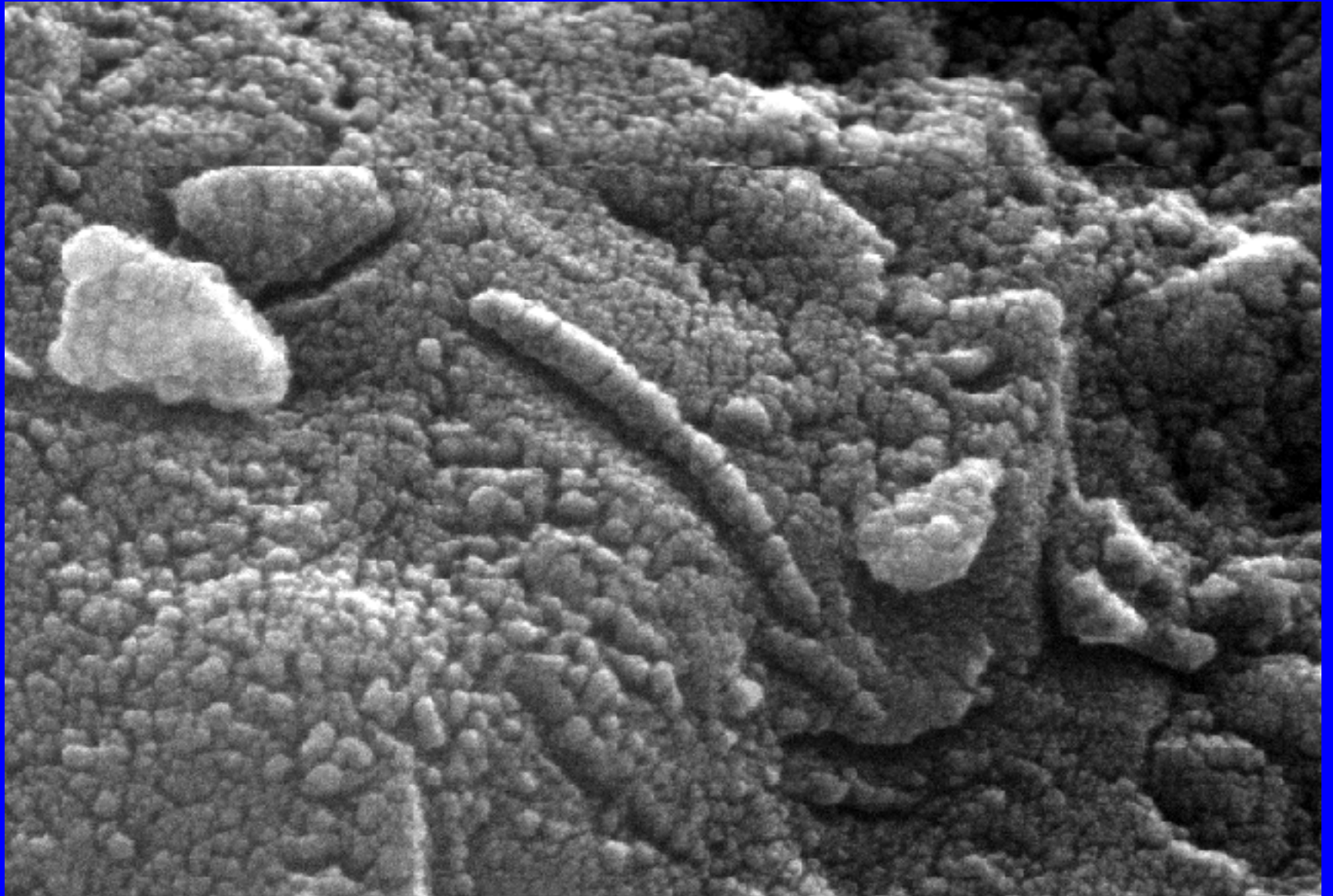
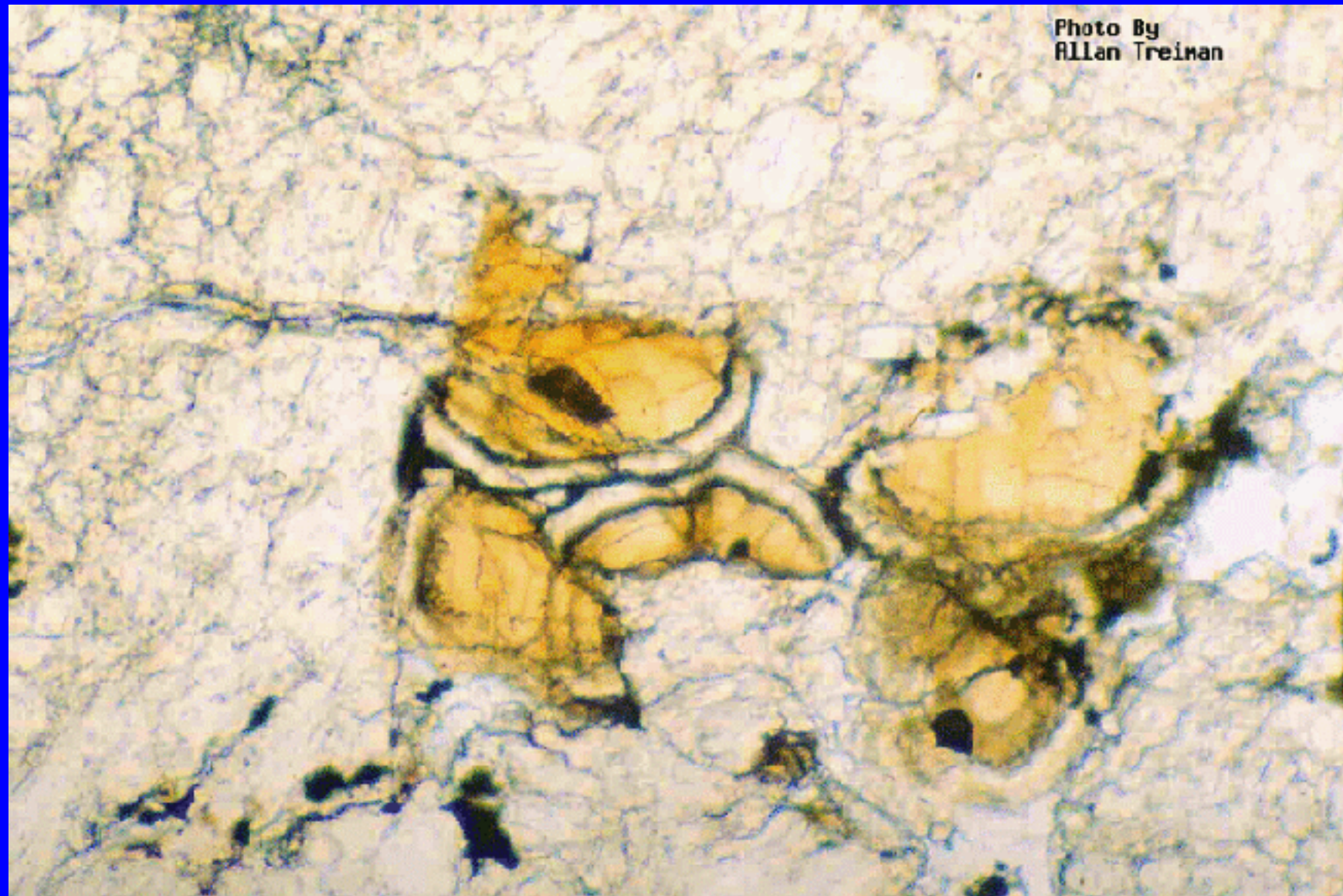


Photo By
Allan Treiman



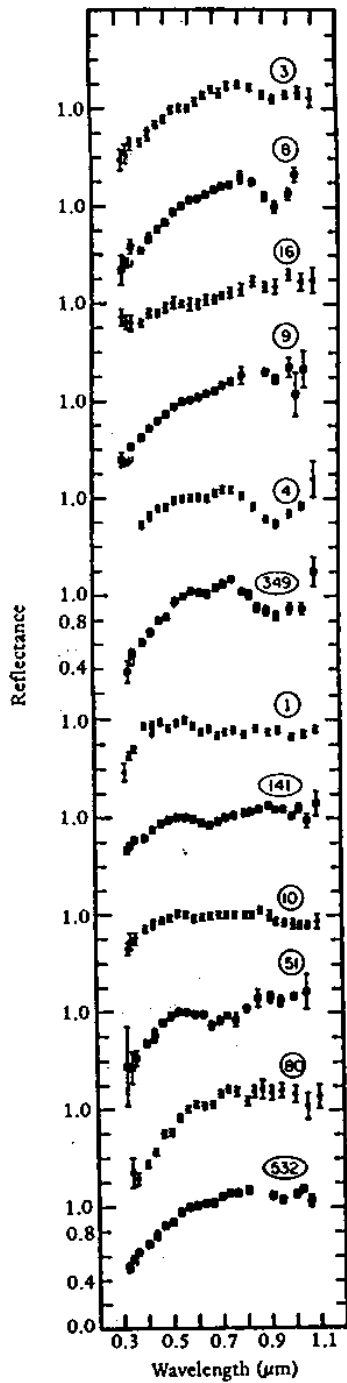


Fig. 3.5. Illustrated here are the reflectance spectra for 12 asteroids. Each of these curves is a composite of overlapping spectra for different minerals. The circled numbers refer to catalog numbers of asteroids: 3 Juno, 8 Flora, 16 Psyche, 9 Metis, 4 Vesta, 349 Dembowska, 1 Ceres, 141 Lumen, 10 Jygiea, 51 Nemansr, 80 Sappho, and 532 Herculina. Included in this list are representatives of most of the different spectral types of asteroids.

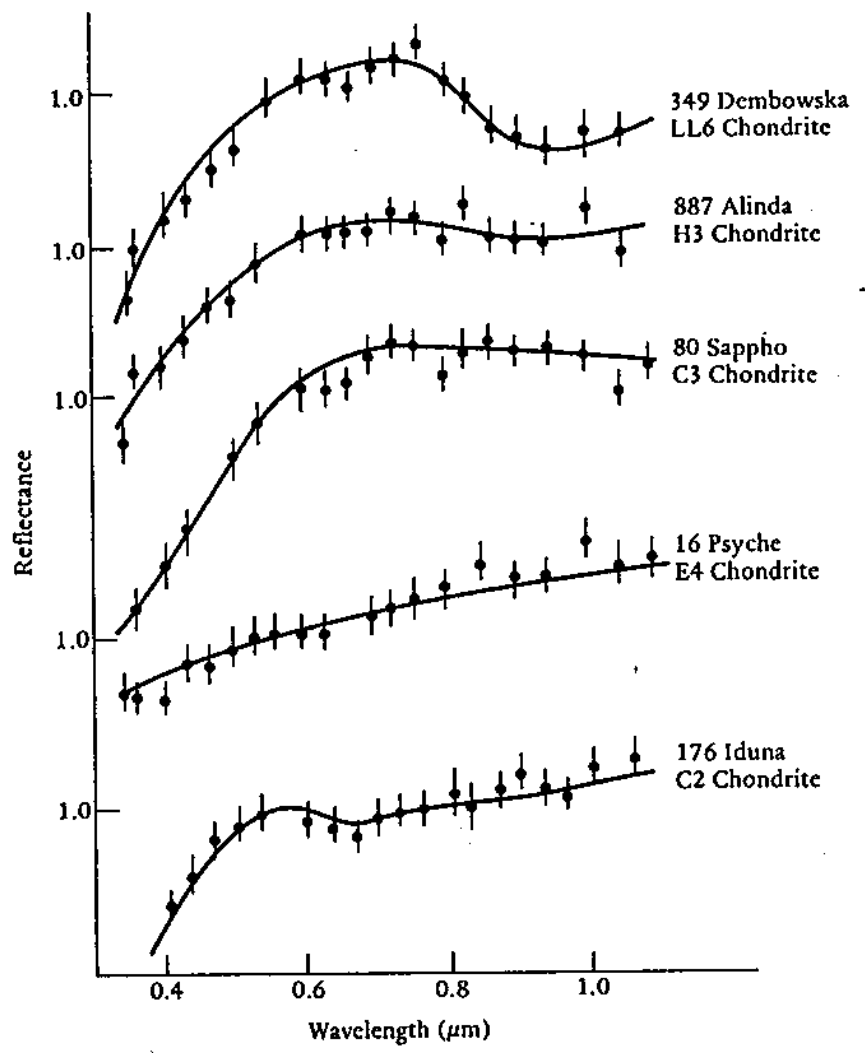


Fig. 3.6. In order to try to identify the compositions of asteroids, comparisons are made between asteroidal and meteorite reflectance spectra. This diagram illustrates five such comparisons between selected asteroids (dots with analytical error bars) and certain classes of chondrites (curves). Because absolute albedo depends on particle sizes, which are unknown in the case of asteroids, it is permissible to translate asteroidal spectra up or down in the diagram in order to obtain a match. All data are therefore arbitrarily assigned an albedo value of 1.0 at a wavelength of 0.56 micrometer.

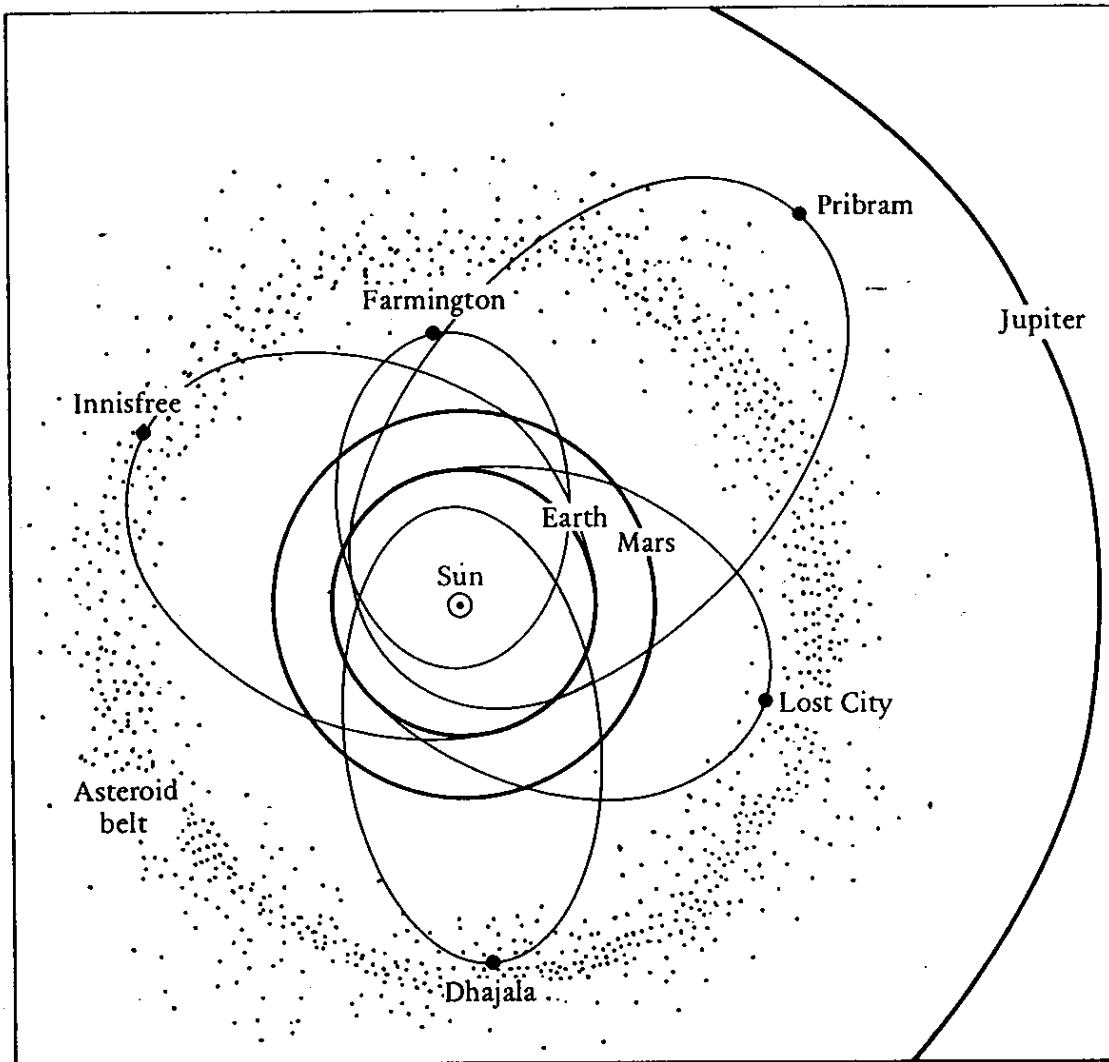


Fig. 3.2. The calculated orbits of recovered meteorites provide information on the sources of these objects. Five recovered ordinary chondrites had highly elliptical orbits. All of these had aphelia, the approximate locations of which are illustrated by small dots in this figure, in or near the asteroid belt between Mars and Jupiter. This suggests that chondrites may be fragments of asteroids. The orbits are drawn to scale, but their orientations are chosen for clarity of illustration.

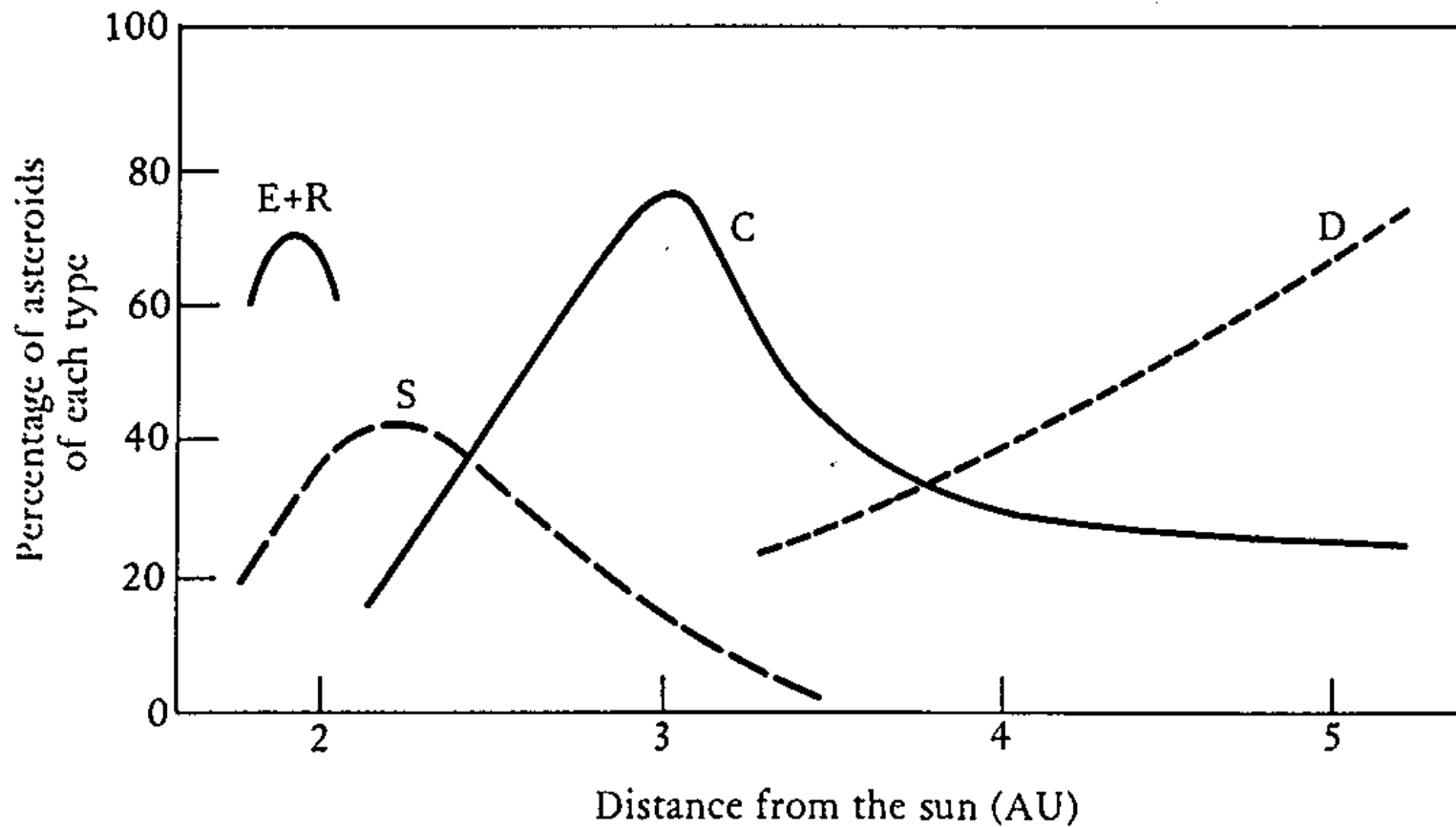
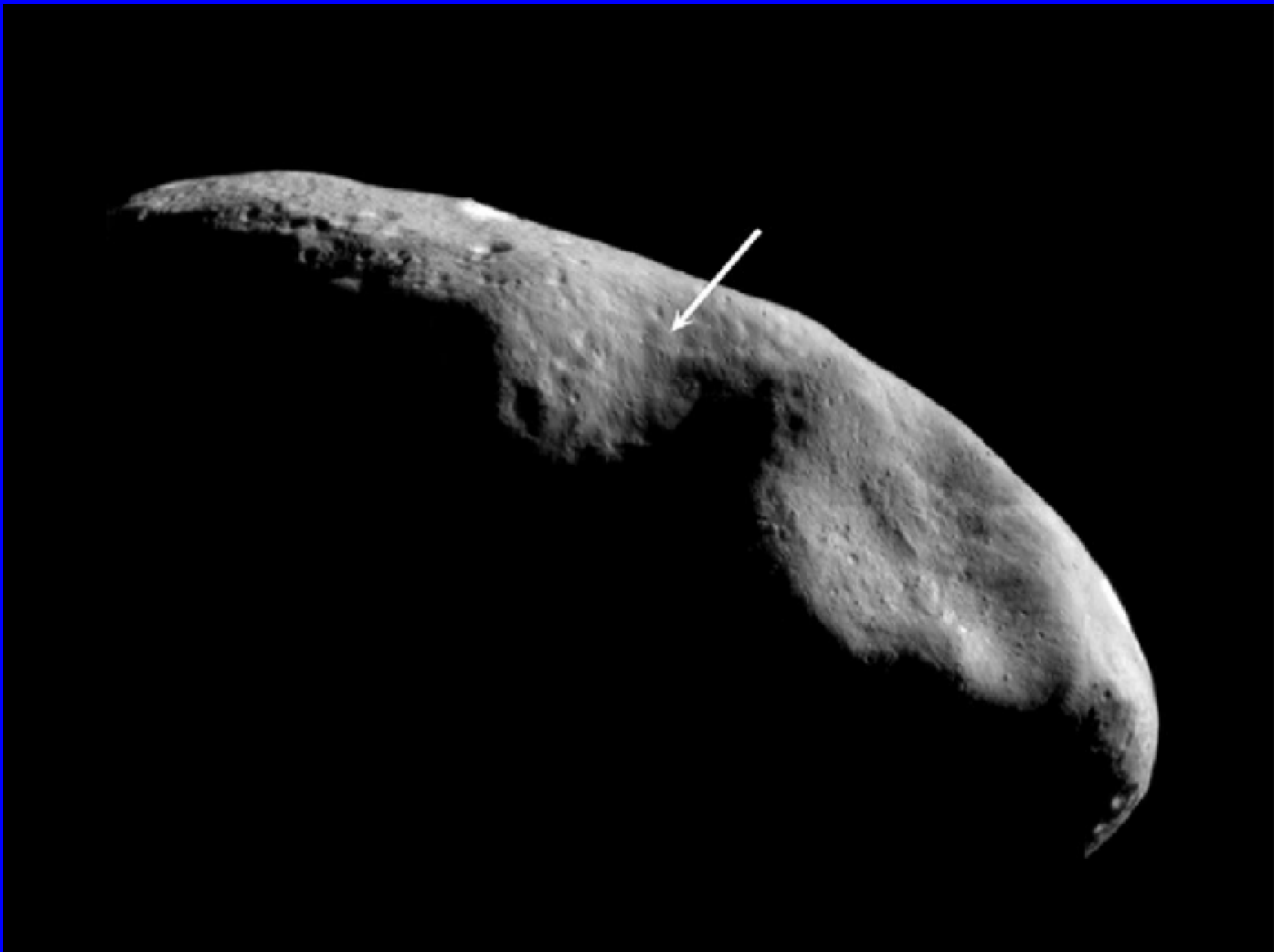


Fig. 3.7. Synthesis of all the available reflectance spectra suggests that the proportions of different asteroid types vary systematically with distance from the sun. E and R types, which are possible enstatite chondrite parent bodies, are located in the inner fringe of the asteroid belt. Ordinary chondrites may be derived from S-type asteroids that tend to occur slightly farther out. C and D types occur primarily in the outer belt and may be the sources of carbonaceous chondrites.

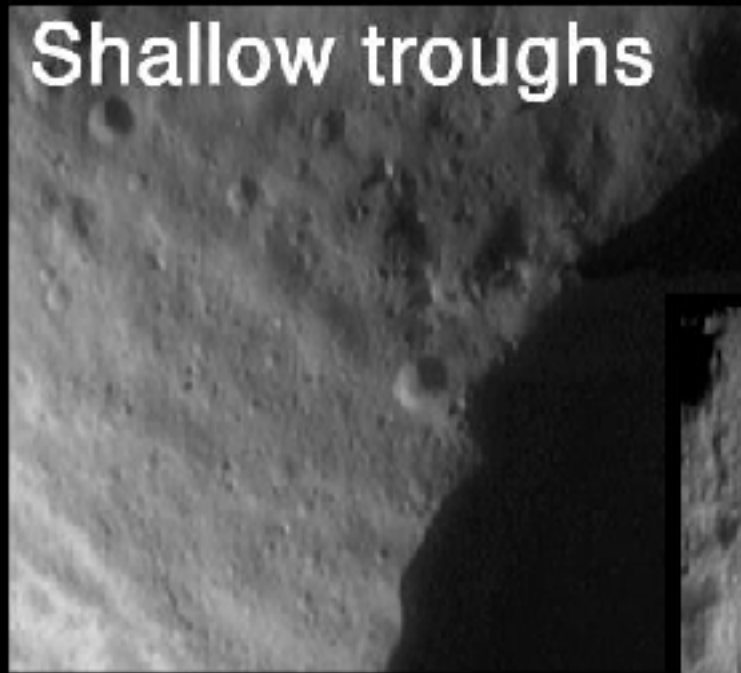








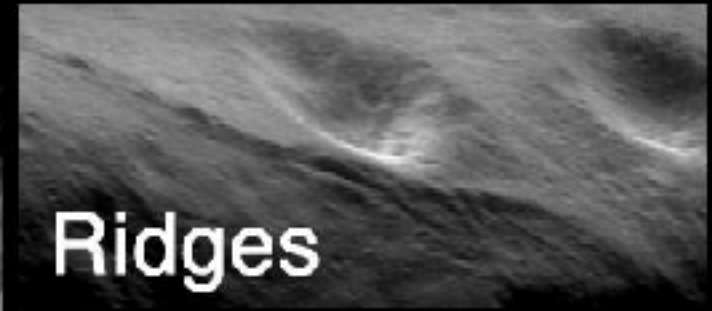
Shallow troughs



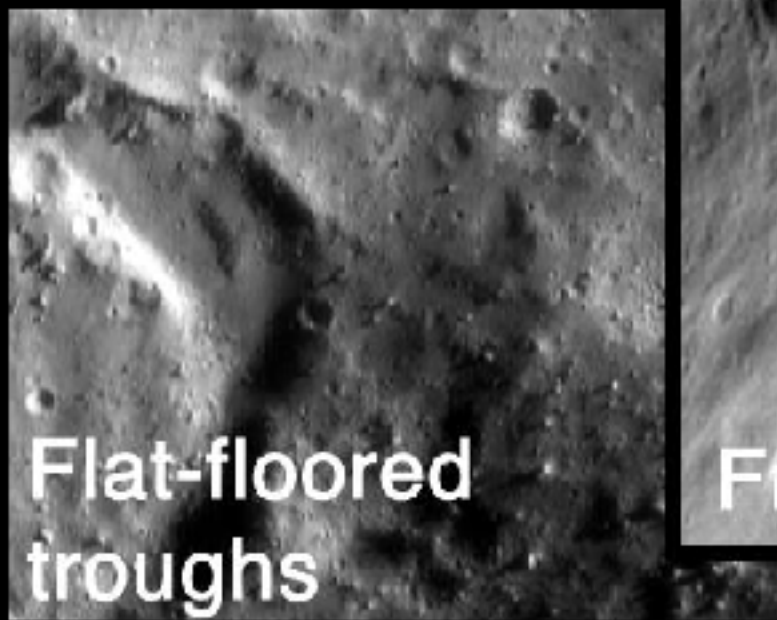
Pit chains



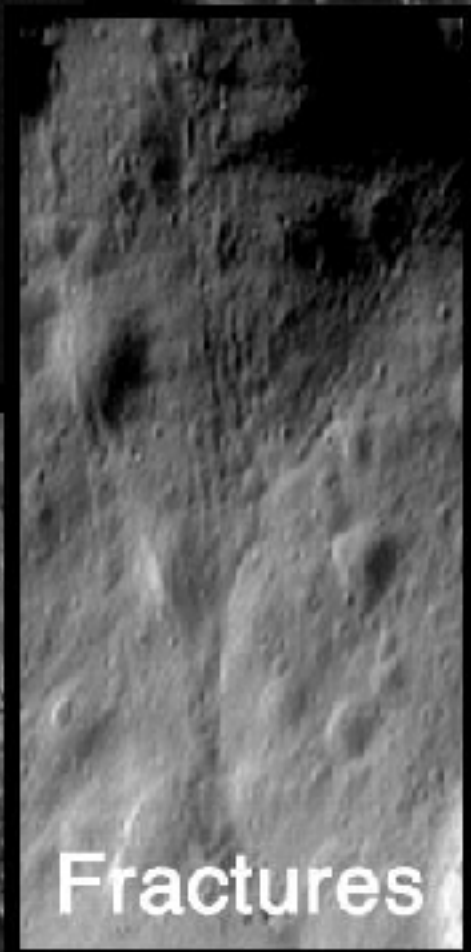
Ridges



**Flat-floored
troughs**



Fractures



Grooves













